

Formation of the cosmic-ray halo: The role of nonlinear Landau damping

D. O. CHERNYSHOV,¹ V. A. DOGIEL,¹ A. V. IVLEV,² A. D. ERLYKIN,¹ AND A. M. KISELEV¹

¹*I. E. Tamm Theoretical Physics Division of P. N. Lebedev Institute of Physics, 119991 Moscow, Russia*

²*Max-Planck-Institut für extraterrestrische Physik, 85748 Garching, Germany*

ABSTRACT

We present a nonlinear model of self-consistent Galactic halo, where the processes of cosmic ray (CR) propagation and excitation/damping of MHD waves are included. The MHD-turbulence, which prevents CR escape from the Galaxy, is entirely generated by the resonant streaming instability. The key mechanism controlling the halo size is the nonlinear Landau (NL) damping, which suppresses the amplitude of MHD fluctuations and, thus, makes the halo larger. The equilibrium turbulence spectrum is determined by a balance of CR excitation and NL damping, which sets the regions of diffusive and advective propagation of CRs. The boundary $z_{\text{cr}}(E)$ between the two regions is the halo size, which slowly increases with the energy. For the vertical magnetic field of $\sim 1 \mu\text{G}$, we estimate $z_{\text{cr}} \sim 1 \text{ kpc}$ for GeV protons. The derived proton spectrum is in a good agreement with observational data.

Keywords: cosmic rays – Galaxy: halo – MHD-turbulence

1. INTRODUCTION

The problem of the Galactic halo is being discussed from the beginning of the 1950s. Before that time, a sharp transition was assumed between the Galactic disk of the thickness of $\sim 100 \text{ pc}$ and the extragalactic medium. Later, Ginzburg (1953) developed conceptions of the physical cosmic ray (CR) halo with the size of about 15 kpc, where CRs are trapped by scattering (i.e., propagate diffusively). The characteristic CR age in the Galaxy was estimated as $\sim 10^8 \text{ yr}$, which is confirmed by radio data and by the information on CR chemical composition (e.g., about the abundance of unstable isotope ^{10}Be) (see, e.g., Ginzburg & Ptuskin 1976; Szabelski et al. 1980, etc.).

The static halo model of a fixed height was presented in Ginzburg & Syrovatskii (1964). It assumes that the CR density at a certain distance from the Galactic plane becomes negligible. This model is currently broadly implemented in advanced numerical codes, such as GALPROP (Moskalenko & Strong 1998).

The downside of the model is that it depends on two arbitrary parameters, namely the diffusion coefficient and the halo size, whose values are ambiguously defined. Therefore, it is necessary to describe the processes of generation and damping of MHD turbulence in the halo and their connections to the CR transport self-consistently.

In Dogiel et al. (2020), we have suggested a model of CR self-confinement in the Galaxy, where the turbulence generated in the Galactic disk was amplified by streaming CRs. However, the turbulence excitation rate is very high in that model, and hence the size of the halo is too small at GeV energies. To resolve this issue, in the present paper we also take into account the nonlinear Landau (NL) damping, which was neglected in the original work. We show that the inclusion of the damping term leads to a significantly larger halo size. We also show that the MHD turbulence which confines CRs in the halo can be entirely self-generated by CRs.

2. SELF-CONSISTENT NONLINEAR MODEL OF CR HALO

Unlike models with a pre-defined halo size, self-consistent halo models include a mechanism of MHD-wave excitation. In these models, CR propagation is described by a system of nonlinear equations (see, e.g., in Dogiel et al. 1994; Evoli et al. 2018; Dogiel et al. 2020, and references therein).

A general system of simplified one-dimensional nonlinear equations for the CR spectrum $N(p, z)$ and the energy density of MHD fluctuations $W(k, z)$ can be presented in the following form:

$$\begin{aligned} \frac{\partial}{\partial z} \left(u_{\text{adv}} N - D \frac{\partial N}{\partial z} \right) - \frac{\partial}{\partial p} \left(\frac{1}{3} \frac{du_{\text{adv}}}{dz} p N - \dot{p} N \right) &= Q, \\ \frac{\partial u_{\text{A}} W}{\partial z} - \frac{du_{\text{A}}}{dz} \frac{\partial(kW)}{\partial k} + \frac{\partial}{\partial k} \left(\frac{kW}{\tau_{\text{cas}}} \right) &= (\Gamma_{\text{CR}} - \nu) W, \end{aligned} \quad (1)$$

where $Q(p, z)$ is the source term of CRs, $u_{\text{adv}}(z)$ is the CR advection velocity, which depends on the difference between outward- and inward-propagating MHD waves, $u_A(z) = B(z)/\sqrt{4\pi\rho(z)}$ is the Alfvén velocity, $\dot{p} < 0$ is the rate of momentum loss due to interaction with gas, $\rho = m_p n$ is the mass density of ionized hydrogen (m_p is proton mass), and B is the strength of the longitudinal large-scale magnetic field. Furthermore, $\Gamma_{\text{CR}}(k, z)$ is the rate of resonant wave excitation, ν is the wave damping rate, and $\tau_{\text{cas}}(W)$ is the characteristic timescale of turbulent cascade to larger k ; the latter depends on the particular process of MHD-generation (see, e.g., [Ptuskin et al. 2006](#), this process is discussed in Section 2.1). The spectrum $N(p, z)$ is normalized such that $\int N(p) dp$ is the total number density of CRs.

The wavenumber k of MHD fluctuations is related to the CR momentum p via the resonance condition ([Skilling 1975](#)),

$$kp \approx m_p \Omega_*, \quad (2)$$

where $\Omega_* = eB/m_p c$ is the gyrofrequency of non-relativistic CR protons. The resulting CR diffusion coefficient is ([Skilling 1975](#))

$$D(p, z) \approx \frac{vB^2}{6\pi^2 k^2 W}. \quad (3)$$

In this approximation, the excitation rate is proportional to the CR diffusion flux,

$$\Gamma_{\text{CR}}(k, z) \approx -\frac{2\pi^2 e u_A p}{Bc} D \frac{\partial N}{\partial z}. \quad (4)$$

There are very few known parameters and processes that can govern the density of MHD-fluctuations in the halo (and thus the CR diffusion). These are the spatial dependencies of the magnetic field and the gas density, the magnitude and the spectrum of CR source in the disk, and nonlinear processes involving MHD waves. In this respect, the variety of models for the wave excitation in the halo is very restricted.

2.1. Development of [Dogiel et al. \(2020\)](#)

[Evoli et al. \(2018\)](#) and [Dogiel et al. \(2020\)](#) presented one-dimensional models of CR propagation along the magnetic field lines, with MHD-fluctuations excited by the resonant CR-streaming instability.

[Evoli et al. \(2018\)](#) developed a model of MHD-turbulence with nonlinear cascading to larger k . They considered three sources of waves responsible for CR scattering in the halo: (i) self-generated MHD-waves excited by CRs through the streaming instability, (ii) processes mimicking wave generation by, e.g., supernova explosions in the disk which eject waves at large scales, and (iii) cascading process which is determined by an initial arbitrary source of background turbulence distributed over the halo. In case the cascading is responsible for the damping of MHD-fluctuations in the halo, the CR

halo can be about of few kpc, which is compatible with the estimations of GALPROP.

On the contrary, [Dogiel et al. \(2020\)](#) showed that the cascading process in the halo is negligible for relevant values of k , i.e., the term containing τ_{cas} in the second Equation (1) can be omitted. We considered two sources of waves responsible for CR scattering in the halo, namely, (i) self-generated MHD waves excited by CRs through the streaming instability, and (ii) the spectrum of MHD-fluctuations generated by sources in the Galactic disk. In that model, magnetic fluctuations are only excited in the direction away from the disk. However, the resulting CR flux excites waves too efficiently, which yields the halo size of only ~ 100 pc at low energies.

In [Dogiel et al. \(2020\)](#), we have not considered the possibility that outgoing waves may be reflected by a nonuniform medium (see [Ferraro 1954](#); [Kulsrud 2005](#), for details). In fact, that happens if the approximation of geometrical optics is no longer applicable. According to [Ginzburg \(1970\)](#), if the wave phase velocity changes from u_{min} to u_{max} within a layer of thickness ℓ , the reflection coefficient R of the outgoing waves from the layer is

$$R^2 \sim \exp\left(-4\pi k \ell \frac{u_{\text{min}}}{u_{\text{max}}}\right). \quad (5)$$

Applying this expression to the halo with $\ell = 1$ kpc, we see that even for very long waves, resonant with PeV protons, only $\sim 0.1\%$ of the total energy is reflected. Therefore, we indeed can safely assume that there are no backward-moving waves present in the halo.

Another physical process neglected in [Dogiel et al. \(2020\)](#) is nonlinear Landau (NL) damping. A two-dimensional halo model including this process has already been developed by [Dogiel et al. \(1993\)](#) and [Dogiel et al. \(1994\)](#). The authors used the equation for CR propagation complemented with the equation for MHD-fluctuations which are excited by the CR flux and attenuated by the NL damping, cascading, and adiabatic losses. It was shown that CR distribution is quasi-isotropic near the Galactic plane, but becomes more focused along the radial coordinate as particles propagate further away. At some point the scattering becomes unable to reflect particles back, which sets the outer boundary of the halo. The halo size was estimated to be about 10 kpc. However the advective transport of CRs was not taken into account in this model.

According to [Völk & Cesarsky \(1982\)](#) and [Miller \(1991\)](#), the rate of NL damping is given by

$$\nu_{\text{NL}}(k) \approx g(n, T) \frac{8\pi u_A}{B^2} k \int_{k_{\text{min}}}^k W(k_1) dk_1, \quad (6)$$

where the lower integration limit k_{min} is unimportant for our self-consistent model (see Section 4.2). Follow-

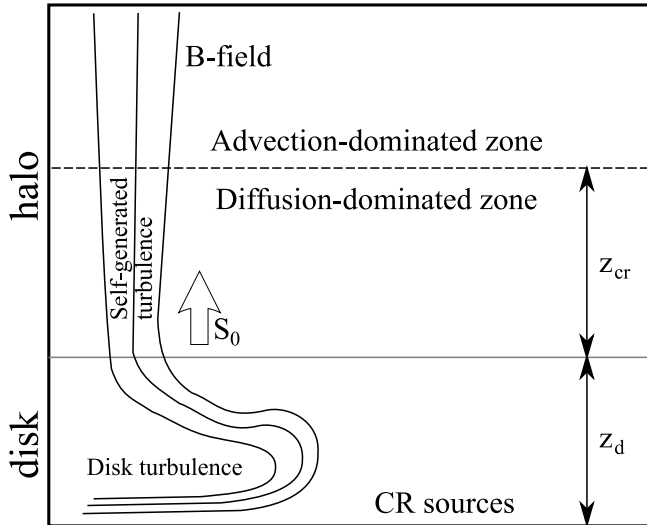


Figure 1. Schematic representation of the model considered in the paper.

ing Miller (1991), the dimensionless factor $g(\beta)$ in Equation (6) can be approximated by

$$g(\beta) \approx \frac{\sqrt{\pi}}{4} \beta^{1/2} \left(e^{-\beta^{-1}} + \frac{1}{2} \epsilon^{1/2} e^{-\epsilon \beta^{-1}} \right). \quad (7)$$

Here, $\epsilon = m_e/m_p$ is electron-to-proton mass ratio and

$$\beta = \frac{nkT}{B^2/8\pi} \equiv \frac{u_{\text{th}}^2}{u_A^2}, \quad (8)$$

is the plasma- β parameter expressed via the thermal velocity of protons u_{th} . We assume that temperatures T of both protons and electrons are equal.

The idea that the excitation of MHD turbulence in a halo can be balanced by NL damping has been previously discussed by Ptuskin et al. (1997). In the present work, we use a different expression for NL damping, which takes into account contributions of both thermal protons and electrons. Furthermore, in our model β significantly drops with the height, which results in a much weaker damping for waves excited by CRs with energies above 100 GeV and, thus, helps to confine such particles.

3. THE HALO MODEL WITH NL DAMPING

The idealized structure of our model is sketched in Figure 1. We consider two characteristic regions along the z -axis: the Galactic disk, where MHD-turbulence is assumed to be generated by sources distributed over the Galactic plane, and the CR halo, where the turbulence is self-generated by the outgoing CR flux. We assume that the magnetic field is practically vertical in the halo (while its geometry can be arbitrary in the disk), and that CRs do not diffuse across the magnetic field lines.

This model allows us to reduce the set of equations (1) to

$$\frac{\partial}{\partial z} \left(u_{\text{adv}} N - D \frac{\partial N}{\partial z} \right) - \frac{\partial}{\partial p} \left(\frac{1}{3} \frac{du_{\text{adv}}}{dz} p N - \dot{p} N \right) = 2Q(p)\delta(z), \quad (9)$$

$$\frac{\partial v_A W}{\partial z} - \frac{du_A}{dz} \frac{\partial k W}{\partial k} = (\Gamma_{\text{CR}} - \nu_{\text{NL}}) W, \quad (10)$$

where $Q(p)$ is the source of CRs above/below the Galactic plane, $\dot{p} < 0$ is the momentum loss rate due to ionization or proton-proton collisions within the disk ($0 < z < z_d$), while in the halo ($z \geq z_d$) the CR losses are solely due to adiabatic cooling. Here and below, z_d is the characteristic height of the disk. The CR advection velocity changes discontinuously at the disk boundary,

$$u_{\text{adv}}(z) = u_A \theta(z - z_d), \quad (11)$$

where $\theta(z)$ is the Heaviside function. We assume that sources of the turbulence in the disk do not contribute to the turbulence in the halo, i.e.

$$W(k, z_d) = 0, \quad (12)$$

i.e., the halo turbulence is entirely self-generated by CRs. However, the existence of turbulence within the disk is essential (Evoli et al. 2018; Dogiel et al. 2020), and we take this into account in Section 4.

According to Equation (7), MHD-waves are damped on plasma electrons in a low- β plasma, and on protons in a high- β plasma. Most of the thermal electrons or protons contribute to the damping if, respectively,

$$0.01 \leq \beta \leq 0.2, \quad (13)$$

or

$$\beta \geq 10. \quad (14)$$

For these values of β , the respective dominant exponential factor in Equation (7) can be set to unity, and ν_{NL} in Equation (6) becomes independent of the plasma density.

Below in Section 4 we obtain a simplified analytical solution of Equations (9) and (10), while in Section 5 we present and discuss the exact numerical solution.

4. ANALYTIC APPROXIMATION

In this section we derive an analytical solution which qualitatively explains the role of NL damping in the self-consistent halo model.

4.1. CR spectrum in the disk, and CR flux from the disk to the halo

To simplify CR propagation in the disk (see, e.g. Berezhinskii et al. 1990), we consider the following two key parameters: the outgoing CR flux and CR distribution function at the boundary between the disk and the halo. They both should be continuous at boundary.

A general equation for the outgoing flux $S_0(p) = S(p, z_d)$ at the boundary is obtained by integrating Equation (9),

$$S_0(p) = Q(p) + \frac{d}{dp} \left(\frac{1}{3} u_{A0} p N_0(p) - \int_0^{z_d} \dot{p} N(z, p) dz \right), \quad (15)$$

where $u_{A0} = u_A(z_d)$ and $N_0(p) = N(p, z_d)$. The flux S_0 derived from Equation (15) can be considered as the boundary condition for Equation (9) at $z = z_d$. Since the halo size should be much larger than z_d , we assume that the CR spectrum does not change significantly across the disk. Then we can approximate $N(p, z) \approx N_0(p)$ for $0 \leq z \leq z_d$.

As pointed out in Dogiel et al. (2020), energy losses in the halo are unimportant and thus the CR flux $S_0(p)$ is conserved. Then we obtain the following solution of Equation (9) for $z \geq z_d$:

$$N(p, z) = \frac{S_0(p)}{u(p, z)}, \quad (16)$$

where $u(p, z)$ is the outflow velocity of CRs,

$$u = \left(\int_{\eta}^{\eta_{\infty}} \frac{e^{\eta - \eta_1} d\eta_1}{u_A(\eta_1)} \right)^{-1}, \quad (17)$$

and $\eta(p, z)$ is a dimensionless variable

$$\eta = \int_{z_d}^z \frac{u_A}{D} dz_1. \quad (18)$$

The value of η_{∞} generally depends on the boundary condition at $z \rightarrow \infty$. Substituting $N_0(p) = N(p, z_d)$ from Equation (16) in Equation (15), we derive the flux,

$$S_0(p) = \frac{u_d(p)}{\mathcal{E}(p)} \int_p^{\infty} Q(p_1) \exp \left(- \int_p^{p_1} \frac{u_d(p_2)}{\mathcal{E}(p_2)} dp_2 \right) dp_1. \quad (19)$$

Here, $u_d(p) = u(p, z_d)$ and $\mathcal{E}(p) = \frac{1}{3} p u_{A0} - \int_0^{z_d} \dot{p} dz = \frac{1}{3} p u_{A0} + \frac{1}{2} \mathcal{N}_H L(p)$, where \mathcal{N}_H is the vertical column density of hydrogen atoms in the disk and $L(p) = -\dot{p}/n_H$ is energy loss function (per unit column density) due to interaction with the disk gas. We note that u_d in fact depends on S_0 , and, therefore, Equation (19) is an integral equation for $S_0(p)$. If the dependence u_d versus S_0 is weak, the equation can be solved iteratively.

We can obtain a simple approximation for $S_0(p)$ assuming that $\mathcal{E} S_0 / u_d$ is a power-law function $\propto p^{-\alpha}$. According to experimental data, $S_0 / u_d \equiv N(p)$ has a negative spectral index smaller than that of $S_0(p)$ (both are smaller than -2), while \mathcal{E} cannot increase faster than

$\propto p$. Therefore, $\alpha > 0$ and we readily obtain from Equation (15),

$$S_0(p) = \frac{Q(p)}{1 + \alpha \mathcal{E} / (p u_d)}. \quad (20)$$

We notice that both the energy loss rate \mathcal{E}/p and the inverse outflow velocity $u_d^{-1} = N/S_0$ decrease with p , and therefore $S_0(p) \approx Q(p)$ for sufficiently high energies. To evaluate a critical energy where $\mathcal{E}/(p u_d) = 1$, we assume $\mathcal{N}_H \approx 6 \times 10^{20} \text{ cm}^{-2}$ and $u_d \sim u_A \sim 10^6 \text{ cm/s}$. This yields the proton energy about 0.5 GeV, above which we can set $S_0 = Q$.

As discussed in Dogiel et al. (2020), the value of η is the key parameter characterizing CR propagation in the halo. The entire halo can be approximately split into two regions: one is called the *halo sheath*, where $\eta(z) \ll 1$ and the diffusion term $-D \partial N / \partial z$ dominates in the CR flux S_0 ; the other is where $\eta(z) \gg 1$ and the advection term $u_{\text{adv}} N$ dominates. The critical point $z_{\text{cr}}(p)$ separating these two regions can be determined from the condition $\eta(p, z_{\text{cr}}) \approx 1$. Since the dominant advection irreversibly carries CRs away from the disk, the halo size can be set equal to z_{cr} . Therefore, the boundary condition at $z \rightarrow \infty$ becomes unimportant as long as $\eta_{\infty} \gg 1$.

In order to derive η from Equation (18), we need to obtain the diffusion coefficient D from Equation (3), which requires the solution of Equation (10).

4.2. Excitation-damping balance

The numerical solution of Equations (9) and (10) (see Section 5) suggests that $W(k, z)$ in the diffusion region can be estimated from the excitation-damping balance,

$$\Gamma_{\text{CR}} = \nu_{\text{NL}}. \quad (21)$$

We rewrite it using Equations (4) and (6),

$$\frac{4g(z)c^2}{\pi e^2 B^2} k^2 \int_{k_{\text{min}}}^k W(k_1) dk_1 = S_0(p) - u_A N. \quad (22)$$

In the halo sheath ($\eta < 1$) the last term of Equation (22) can be neglected. In this case, $S_0(p) \propto Q(p)$ decreases with p faster than p^{-2} , and thus the integral on the left-hand side of Equation (22) is dominated by the upper limit k . Therefore,

$$W(k, z) = \frac{\pi}{4g(z)} \frac{\partial}{\partial k} [p^2 S_0(p)], \quad (23)$$

and

$$\eta(p, z) = - \frac{3\pi^3 e}{2vc} \frac{\partial}{\partial p} [p^2 S_0(p)] \int_{z_d}^z \frac{u_A}{B g(z_1)} dz_1. \quad (24)$$

From Equation (7) we obtain

$$\eta = -\frac{6\pi^{5/2}e}{vc} \frac{\partial}{\partial p} [p^2 S_0(p)] \int_{z_d}^z \frac{u_{\text{th}}(T)\beta^{-1} dz_1}{B(e^{-\beta^{-1}} + \frac{1}{2}\epsilon^{1/2}e^{-\epsilon\beta^{-1}})}. \quad (25)$$

For simplicity, below we assume $n(z) = n_0 \exp(-z/z_n)$, $B(z) = B_0 \exp(-z/z_B)$, and $T(z) = T_0 \exp(z/z_T)$.

4.3. Spectrum of CRs in the halo sheath

If β is within the ranges defined in Equations (13) and (14), the expression for $g(\beta)$ simplifies significantly. In this regime, previously considered by Ptuskin et al. (1997), we can neglect the exponential dependence in the denominator of Equation (25) and rewrite the equation as

$$\eta(p, z) = A(p) \left(e^{z/z_n} - e^{z_d/z_n} \right), \quad (26)$$

where $z_n^{-1} = z_n^{-1} - z_B^{-1} - \frac{1}{2}z_T^{-1}$. For the sake of simplicity, below we assume $z_d \approx 0$.

The magnitude of the dimensionless factor $A(p)$ depends on the dominant mechanism of NL damping. In a low- β plasma with $0.01 \leq \beta \leq 0.2$ the damping on thermal electrons dominates, and

$$A(p) \approx A_e(p) = -\frac{12\pi^{5/2}eu_{A0}^2 z_\eta}{vcB_0 u_{\text{th}0} \epsilon^{1/2}} \frac{\partial}{\partial p} [p^2 S_0(p)], \quad (27)$$

where $u_{\text{th}0} = u_{\text{th}}(z_d)$, while in a high- β plasma with $\beta \geq 10$ the damping is due to thermal protons, and

$$A(p) \approx A_p(p) = \frac{1}{2}\epsilon^{1/2} A_e(p). \quad (28)$$

The critical point z_{cr} is derived from the condition $\eta \approx 1$. Thus, the halo size is estimated from Equation (26) as

$$z_{\text{cr}}(p) = z_\eta \ln [1 + 1/A(p)]. \quad (29)$$

For low energies, where $A(p) \gg 1$, the halo size increases with p as $z_{\text{cr}}(p) \approx z_\eta/A(p)$; for high energies, the halo size $z_{\text{cr}}(p) \approx -z_\eta \ln A(p)$ is almost independent of p . We point out that the model is not viable in the former regime, normally corresponding to the electron-dominated damping, because the resulting halo size becomes too small. On the other hand, for the proton-dominated damping with $\beta > 10$, the function $A_p(p) \sim 1$ for the following halo parameters: $B \leq 1 \mu\text{G}$, $n \geq 10^{-2} \text{ cm}^{-3}$, and $T \geq 100 \text{ eV}$. The halo size in this case exceeds 1 kpc at energies above 1 GeV.

The CR spectrum is given by Equation (16),

$$N(p, z) = \frac{S_0(p)}{u_{A0}} \int_\eta^\infty \frac{e^{\eta-\eta_1} d\eta_1}{[1 + \eta_1/A(p)]^{z_\eta/z_A}}, \quad (30)$$

where $z_A^{-1} = \frac{1}{2}z_n^{-1} - z_B^{-1}$ characterizes the spatial scale of variation of $v_A(z)$. This result can be expressed in

terms of the incomplete gamma-function $\Gamma(a, z)$,

$$N(p, z) = \frac{S_0(p)}{u_{A0}} e^{\eta+A(p)} A(p)^{z_\eta/z_A} \times \Gamma(1 - z_\eta/z_A, A(p) + \eta). \quad (31)$$

If $A(p) + \eta \gg 1$, the solution corresponds to the advection flux with the Alfvén velocity at the halo periphery. This represents low-energy CRs at large distances from the disk,

$$N(p, z) \approx \frac{S_0(p)}{u_{A0}} [1 + \eta/A(p)]^{-z_\eta/z_A} = \frac{S_0(p)}{u_{A0}} e^{-z/z_A} \equiv \frac{S_0(p)}{u_A(z)}. \quad (32)$$

If $A(p) + \eta \ll 1$, the CR spectrum tends to

$$N(p, z) \approx \frac{S_0(p)}{u_{A0}} A(p)^{z_\eta/z_A} \Gamma(1 - z_\eta/z_A) \propto S_0(p) [p S_0(p)]^{z_\eta/z_A}. \quad (33)$$

The resulting spectrum, corresponding to the diffusion-dominated flux, does not practically depend on z up to the critical point z_{cr} . We note that Equation (33) resembles Equation (34) from Ptuskin et al. (1997).

The derived approximate solution has important implications. We conclude that CRs escape from the halo at $z = 1 - 10$ kpc, and for energetic CRs the halo size weakly depends on their energy. Given $S_0(p) \propto p^{-2.4}$ and $N(p) \propto p^{-2.7}$, our solution suggests that $z_\eta/z_A \approx 0.3/1.4$ or $z_n/z_B - 0.15z_n/z_T = 0.35$.

5. NUMERICAL SOLUTION AND DISCUSSION

Equations (32) and (33) provide sufficiently good approximations for the CR spectrum as long as β is within the ranges defined in Equations (13) and (14). However, the magnitude of β varies strongly with z and, therefore, the exponential terms in the denominator of Equation (25) cannot be generally ignored. As a result, the expressions for η and N become complicated and can only be obtained numerically.

To reduce the number of free parameters, we consider a simple isothermal model ($z_T^{-1} = 0$) with a constant magnetic field ($z_B^{-1} = 0$). We use the following set of parameters: $B = 1 \mu\text{G}$, $n_0 = 0.1 \text{ cm}^{-3}$, $z_n = 1 \text{ kpc}$, and $T = 10 \text{ eV}$. For the CR source function, we use $Q(p) \simeq Q_*(p/m_p c)^{-2.4}$ with $Q_* m_p c = 9.4 \times 10^{-4} \text{ cm}^{-2} \text{ s}^{-1}$, which is similar to the value given by Strong et al. (2010). In this case, $\beta = 40$ at $z = 0$. The total power of CR sources in the Galaxy can be roughly estimated as $\mathcal{W} = 2\pi R_{\text{Gal}}^2 \int E_{\text{kin}}(p) Q(p) dp = 4.5 \times 10^{-3} \text{ erg} \times 2\pi R_{\text{Gal}}^2 Q_* m_p c$. Assuming $R_{\text{Gal}} = 20 \text{ kpc}$ for the Galactic disk radius, we obtain $\mathcal{W} \approx 10^{41} \text{ erg/s}$.

Equations (9) and (10) are solved numerically by employing the procedure described in Dogiel et al. (2020).

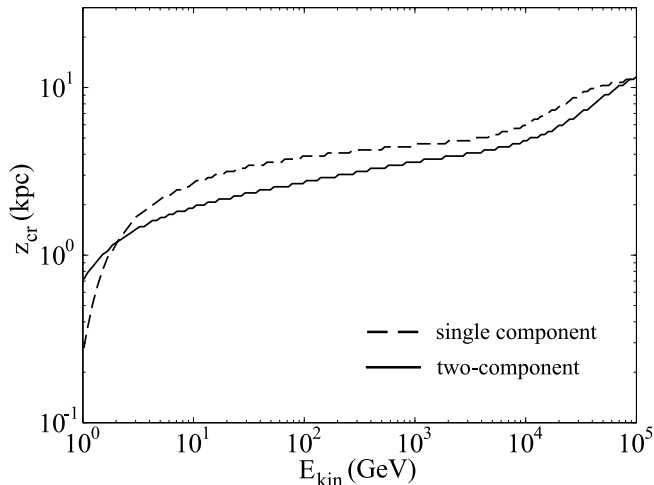


Figure 2. Halo size $z_{\text{cr}}(E_{\text{kin}})$ obtained from the numerical solution of our model. The dashed line shows the case of a single-component gas with $B = 1 \mu\text{G}$, $n_0 = 0.1 \text{ cm}^{-3}$, $z_n = 1 \text{ kpc}$, and $T = 10 \text{ eV}$ ($\beta = 40$), the solid line represents the case of a two-component gas (see Section 5).

To account for CR species heavier than protons, the excitation rate Γ_{CR} is multiplied by a factor of 1.5 (see, e.g., Dogiel et al. 2018). For the initial CR density we use $N(p, z) = 0$, to avoid appearance of a sharp discontinuity at the upper halo boundary. Both the initial MHD spectrum and the boundary condition at $z = 0$ are equal to a small non-zero function $W_0(k, z)$, as it is necessary for the waves excitation. To ensure a weak (logarithmic) dependence of the integral in Equation (6) on the integration limits, we use $W_0(k, z) \propto k^{-1}$.

The resulting halo size, z_{cr} , and the differential CR spectrum, $N/4\pi$, are plotted versus the proton kinetic energy E_{kin} by the dashed lines in Figures 2 and 3, respectively. To account for the solar modulation, we use the force-field approximation with potential $\phi = 0.5 \text{ GV}$ (Gleeson & Axford 1968). Observational data are taken from Aguilar et al. (2015) (AMS-02), Adriani et al. (2019) (CALET), Grebenyuk et al. (2019) (NUCLEON), Yoon et al. (2011) (CREAM-I), Yoon et al. (2017) (CREAM-I+III), and An et al. (2019) (DAMPE). The data are collected using Cosmic-Ray DataBase (CRDB v4.0) by Maurin et al. (2020).

We stress that the CR spectra strongly depend on a particular model of NL damping. In our case, the damping is described by Equations (6) and (7). Since β rapidly drops with the height, so does the damping and, hence, the CR diffusion coefficient. Therefore the CR spectra plotted in Figure 3 can be interpreted as follows:

- $E_{\text{kin}} < 10 \text{ GeV}$: At such energies, $A(p)$ is sufficiently large and, thus, the halo size is small in accordance with Equation (29). For this reason, $\beta(z_{\text{cr}}) \approx \beta(0) > 10$ and NL damping is due to ther-

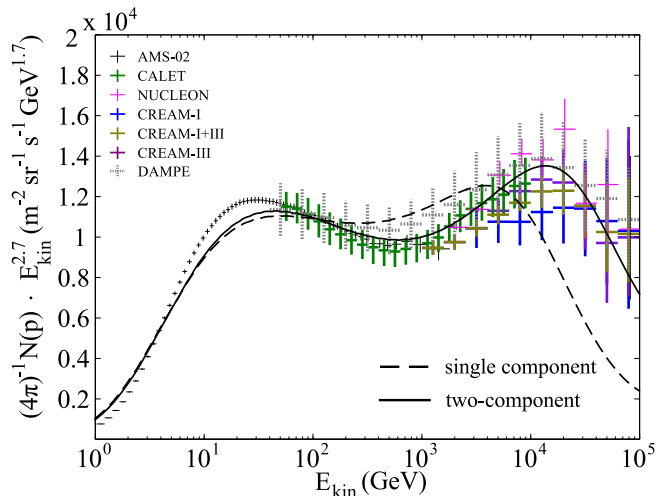


Figure 3. Energy spectra of CR protons obtained from the numerical solution of our model (lines) and the observational data (symbols). All parameters are the same as in Figure 2.

mal protons. Equation (32) is applicable, which gives $N(p) \propto Q(p) \propto p^{-2.4}$.

- $10 \text{ GeV} < E_{\text{kin}} < 1 \text{ TeV}$: $N(p)$ starts approaching a softer spectrum described by Equation (33). The halo size increases with energy as $z_{\text{cr}}(p) \propto 1/A(p)$, and thus $\beta(z_{\text{cr}})$ rapidly decreases, so that eventually a mixed damping both on thermal protons and electrons operates.
- $100 \text{ GeV} < E_{\text{kin}} < 10 \text{ TeV}$: In the mixed-damping regime, a smooth transition from $A_p(p)$ to much larger $A_e(p)$ occurs. According to Equation (33), that makes $N(p)$ harder (NL damping rapidly reduces with CR energy as the proton contribution becomes negligible, and therefore the CR confinement increases). In Figure 3, the transition is manifested by the increase seen at $1 \text{ TeV} < E_{\text{kin}} < 10 \text{ TeV}$.
- $E_{\text{kin}} > 10 \text{ TeV}$: Finally, at very high energies $\beta(z_{\text{cr}})$ decreases below 0.1, where the damping is due to thermal electrons. Equation (33) becomes applicable; since $z_{\eta}/z_A = 1/2$ in our case, $N(p) \propto p^{-3.1}$.

Figure 3 shows that the theoretical curve and the experimental data are in good qualitative agreement. However, we should also keep in mind that gas in the halo consists of several components. In particular, the warm ionized gas (WIM) dominates at lower altitudes, while at higher z it is mostly hot coronal gas (Ferrière 1998; Gaensler et al. 2008). To account for multiple gas components, we assume that the total gas density in our model is determined by a sum of the two phases: $n(z) = n_{\text{hot}}(z) + n_{\text{WIM}}(z)$. The same principle applies to the magnitude of NL damping in Equation (6):

$g(z) = g(\beta_{\text{hot}}) + g(\beta_{\text{WIM}})$. Note that the factor ku_A in Equation (6) is the wave frequency, and therefore is the same in both phases. Assuming $B = 1 \mu\text{G}$, we use the following set of parameters:

- Warm phase ($\beta = 4$): $n_0 = 0.1 \text{ cm}^{-3}$, $T = 1 \text{ eV}$, $z_n = 0.4 \text{ kpc}$.
- Hot phase ($\beta = 4$): $n_0 = 10^{-3} \text{ cm}^{-3}$, $T = 100 \text{ eV}$, $z_n = 2 \text{ kpc}$.

The source function is $Q(p) \simeq Q_*(p/m_p c)^{-2.32}$ with $Q_* m_p c = 9 \times 10^{-4} \text{ cm}^{-2} \text{ s}^{-1}$.

The results for the two-phase model are depicted in Figures 2 and 3 by the solid lines. We see that the theoretical curve show a much better agreement with the observational data in this case, which is due to a much weaker dependence of β on z .

While the two-phase model provides a remarkably good overall agreement with the experimental data in a wide energy range, the discrepancy below 10 GeV is up to 20%. We believe that this is because the effect of disk turbulence on the vertical profile of the spectrum can no longer be ignored at such low energies. Indeed, by deriving Equation (19) we assume that $N(p, z_d) = N(p, 0)$. While this assumption is certainly reasonable for high energies, the low-energy part of the spectrum should be stronger affected by the fact that the diffusion coefficient in the disk decreases with energy, which inevitably leads to an increasing vertical gradient of $N(z)$. Therefore, the low-energy spectrum should be more inhomogeneous at $0 < z < z_d$, and the actual spectrum at $z = 0$ should go somewhat above the theoretical curves plotted in Figure 3. Furthermore, the diffusion coefficient in the Galactic disk is likely not affected by the CR streaming (e.g., due to heavy damping on neutrals), but rather depends on external sources of turbulence (such as supernova explosions and stellar winds).

Apart from the halo size, another important parameter characterizing propagation of CRs is their grammage X , i.e., the average surface density traversed by CRs during their lifetime in the Galaxy. The grammage determines the ratio of secondary-to-primary nuclei, and thus can be derived from experimental data. For our model, it can be roughly estimated as

$$X \approx \mathcal{N}_H m_p \frac{c}{u_d}, \quad (34)$$

which gives $X(10 \text{ GeV}) \approx 12 \text{ g/cm}^2$ for our parameters at $E_{\text{kin}} = 10 \text{ GeV}$. This value is close to that obtained by, e.g., Engelmann et al. (1990). We stress, however, that such estimates are very approximate: to properly test the model, we need to accurately calculate the spectra of secondary and primary nuclei, and compare them to the experimental data. This work will be reported in a separate paper.

6. CONCLUSIONS

We present a development of the self-consistent model of the Galactic CR halo, extending the model by Dogiel et al. (2020). Our earlier model by Dogiel et al. (2020) predicts a small size of the halo at low energies, which does not agree with experimental data. To overcome this discrepancy, we include nonlinear Landau (NL) damping in the present model.

The key input parameters of the proposed model are the CR source $Q(p)$ as well as the spatial profiles of the vertical magnetic field B , ionized gas density n , and temperature T . We show that all these parameters may significantly affect the size of the halo, in particular at relatively low CR energies. The MHD-turbulence in the halo, which controls the vertical escape of CRs, is entirely generated by the resonant CR-streaming instability. The equilibrium spectrum of MHD waves in our present model is reached when the CR excitation rate is balanced by NL damping. This significantly suppresses the amplitude of MHD waves compared to the model of Dogiel et al. (2020), thus making the halo size substantially larger.

We consider two alternative models of gas distributions in the halo: a single-component isothermal model and a two-phase model composed of hot coronal gas and warm ionized gas. We showed that the single-component model requires very dense and hot gas with $\beta \approx 40$ at low altitudes to be able to reproduce the experimental data. For the two-phase model, the required gas parameters are much closer to those reported in the literature (e.g., Ferrière 1998).

Our model is able to reproduce the spectrum of CR protons in a wide range of energies, including the spectral features observed between $\sim 10 \text{ GeV}$ and $\sim 10 \text{ TeV}$ (see Fig. 3). Despite some 20% discrepancy with experimental data below 10 GeV, our model predicts a reasonable halo size of about 1 kpc at 1 GeV. We argue that such a discrepancy may be due to increasing influence of the Galactic disk at lower energies, which is still neglected in our model.

ACKNOWLEDGMENTS

The authors are grateful to an anonymous referee for constructive suggestions, and to Andrey Bykov for useful discussions and comments. The work of DOC, VAD, ADE, and AMK is supported by the Russian Science Foundation via the Project 20-12-00047.

NOTE ADDED IN PROOF

New data on CR proton spectrum reported by CALET (Adriani et al. 2022) confirms the existence of the second spectral break at 10 TeV. The break position suggests that the scale height of hot gas should be about 2 kpc or less.

REFERENCES

- Adriani, O., Akaike, Y., Asano, K., et al. 2019, *PhRvL*, 122, 181102
- . 2022, *PhRvL*, 129, 101102
- Aguilar, M., Aisa, D., Alpat, B., et al. 2015, *PhRvL*, 114, 171103
- An, Q., Asfandiyarov, R., Azzarello, P., et al. 2019, *Science Advances*, 5, eaax3793
- Berezinskii, V. S., Bulanov, S. V., Dogiel, V. A., Ginzburg, V. L., & Ptuskin, V. S. 1990, *Astrophysics of cosmic rays* (Amsterdam: North Holland)
- Dogel', V. A., Gurevich, A. V., & Zybin, K. P. 1993, *A&A*, 268, 356
- Dogiel, V. A., Chernyshov, D. O., Ivlev, A. V., et al. 2018, *ApJ*, 868, 114
- Dogiel, V. A., Gurevich, A. V., & Zybin, K. P. 1994, *A&A*, 281, 937
- Dogiel, V. A., Ivlev, A. V., Chernyshov, D. O., & Ko, C. M. 2020, *ApJ*, 903, 135
- Engelmann, J. J., Ferrando, P., Soutoul, A., et al. 1990, *A&A*, 233, 96
- Evoli, C., Blasi, P., Morlino, G., & Aloisio, R. 2018, *PhRvL*, 121, 021102
- Ferraro, V. C. A. 1954, *ApJ*, 119, 393
- Ferrière, K. 1998, *ApJ*, 503, 700
- Gaensler, B. M., Madsen, G. J., Chatterjee, S., & Mao, S. A. 2008, *PASA*, 25, 184
- Ginzburg, V. L. 1953, *Uspekhi Fizicheskikh Nauk*, 51, 343
- . 1970, *The propagation of electromagnetic waves in plasmas*, Commonwealth and International Library (Pergamon Press)
- Ginzburg, V. L., & Ptuskin, V. S. 1976, *Reviews of Modern Physics*, 48, 161
- Ginzburg, V. L., & Syrovatskii, S. I. 1964, *The Origin of Cosmic Rays* (New York: Macmillan)
- Gleeson, L. J., & Axford, W. I. 1968, *ApJ*, 154, 1011
- Grebenyuk, V., Karmanov, D., Kovalev, I., et al. 2019, *Advances in Space Research*, 64, 2546
- Kulsrud, R. M. 2005, *Plasma physics for astrophysics*, Princeton Series in Astrophysics (Princeton University Press)
- Maurin, D., Dembinski, H. P., Gonzalez, J., Mariş, I. C., & Melot, F. 2020, *Universe*, 6, 102
- Miller, J. A. 1991, *ApJ*, 376, 342
- Moskalenko, I. V., & Strong, A. W. 1998, *ApJ*, 493, 694
- Ptuskin, V. S., Moskalenko, I. V., Jones, F. C., Strong, A. W., & Zirakashvili, V. N. 2006, *ApJ*, 642, 902
- Ptuskin, V. S., Voelk, H. J., Zirakashvili, V. N., & Breitschwerdt, D. 1997, *A&A*, 321, 434
- Skilling, J. 1975, *MNRAS*, 173, 255
- Strong, A. W., Porter, T. A., Digel, S. W., et al. 2010, *ApJL*, 722, L58
- Szabelski, J., Wdowczyk, J., & Wolfendale, A. W. 1980, *Nature*, 285, 386
- Völk, H. J., & Cesarsky, C. J. 1982, *Zeitschrift Naturforschung Teil A*, 37, 809
- Yoon, Y. S., Ahn, H. S., Allison, P. S., et al. 2011, *ApJ*, 728, 122
- Yoon, Y. S., Anderson, T., Barrau, A., et al. 2017, *ApJ*, 839, 5